Palladium Sorption on Glutaraldehyde Crosslinked Chitosan in Dynamic Systems

Montserrat RUIZ[(1)], Ana Maria SASTRE[(2)], Maria Celia ZIKAN[(3)], Eric GUIBAL[(3)]*

[(1)] Universitat Politècnica de Catalunya - E.U.P.V.G.
Av. Victor Balaguer, s/n., E-08800 VILANOVA i la GELTRU - SPAIN

[(2)] Universitat Politècnica de Catalunya - E.I.T.S.E.I.
Diagonal 647, E-08028 BARCELONA - SPAIN

[(3)] Ecole des Mines d'Alès - Laboratoire Génie de l'Environnement Industriel
6 avenue de Clavières - F-30319 ALES cedex - FRANCE
Corresp. author: +33 (0)4 66 78 27 34 (Phone) - +33 (0)4 66 78 27 01 (Fax) - Eric.Guibal@ema.fr

Abstract:

Palladium sorption on glutaraldehyde-crosslinked chitosan is studied in fixed-bed column systems. Sorption performances are mainly controlled by the presence of competitor anions in the solution: the presence of sulfate, chloride in excess or nitrate (to a lesser extent) significantly decrease sorption properties. Though the influence of other operating conditions such as particle size, column depth, flow velocity on sorption breakthrough can not be completely neglected, palladium sorption is less significantly controlled by these parameters than the sorption of other systems owing the fast mass transfer and the weak intraparticle diffusion control.

Key Words: chitosan, palladium, sorption, fixed-bed column, particle size, flow velocity, column depth.

Introduction

Palladium is widely used in industry for the synthesis of catalysts. The expensive cost of this metal may explain the number of reserach programmes focused on its recovery from dilute aqueous effluents as well from industrial wastes [1]. Several techniques have been experimented with using adsorption processes, ion exchange techniques, liquid/liquid extraction or more sophisticated processes including impregnated resins, liquid membranes [1-5]. However facing the technical and/or economical limitations of these processes, there is a need for the development of alternatives processes, especially in the case of dilute effluents. Sorption processes using waste materials haven been proposed including fungal biomass [6], or biopolymers [7-8]. Chitosan is one of these new biomaterials which have been screened for metal recovery [9-11] and especially for platinum group metal (PGM) and gold recovery [8,12-15]. Several derivatives of chitosan have been investigated including iminodiacetic acid derivatives [14] or sulfur derivatives [16] for platinum, palladium removal. Chitosan being soluble in many mineral and organic acids, a crosslinking treatment is frequently used to reinforce the stability of the polymer in acidic solutions [17]. Indeed, due to its cationic behaviour in acidic solutions, chitosan is able to sorb metal anions such as molybdate, vanadate, hexachloroplatinate and tetrachloropalladate through anion exchange mechanism between the counter anions and the metal anions and/or electrostatic attraction between protonated amine groups and metal anions [8,14]. These processes are usually strongly controlled by the presence of competitor anions such as chloride, sulfate and to limit their influence on sorption performances, chitosan has been modified by grafting new functional groups in order to transform the ion exchange resin into a chelating resin [16].

Despite the large number of studies on PGM sorption using chitosan, the literature is not really abundant on the optimization of sorption processes regarding sorption isotherms and uptake kinetics. Among the few papers focused on these in-deep investigations, sorption in dynamic systems is rarely studied. This study has been dedicated to the investigation of palladium sorption using fixed-bed columns and glutaraldehyde crosslinked chitosan flakes. A special attention has been paid to the influence of operating conditions such as flow velocity, metal ion concentration, column depth and sorbent particle size. Several models based on fundamental mass transport

mechanisms, including external film, pore and surface diffusion have been proposed but require the solution of a number of differential equations [18-20]. In addition, these solutions also require accurate correlations for mass-transfer parameters to describe external film, internal pore diffusion and the equilibrium relationship between sorbate and sorbent. There are several simplified design models available such as the ved depth service time (BDST), derived from the Bohart and Adams equation [21] and the Hutchins approach [22], the empty bed residence time (EBRT) [23]. These simplified models are used in this study for the optimization of palladium sorption in small fixed-bed columns before the scaling-up of the process.

Material and Methods

Materials

Chitosan was supplied by ABER-Technologie (France) as a flaked material, with a deacetylation percentage ca. 87 %, defined by FTIR spectrometry [11]. The mean molecular weight was measured at 125 000, using a size exclusion chromatography (SEC) method coupled with a differential refractometer and a multi-angle laser light scattering photometer [10]. Moisture content of sorbent particles, for both crosslinked and uncrosslinked sorbents, was determined at ca. 10 %; sorbent masses are expressed on a wet basis except where otherwise noted.

Chitosan Crosslinking

Chemical crosslinking of chitosan chains with the bifunctional reagent glutaraldehyde occurs by a Schiff's reaction of aldehyde groups on glutaraldehyde with amino groups on the chitosan biopolymer chain [23]. The glutaraldehyde crosslinking bath contained concentrations varying between 0.145 and 1.45 M. The ratio of glutaraldehyde to chitosan (crosslinking ratio CR: mol GA / mol NH_2) varied between 0.42 and 4.15. Unless specified, the crosslinking ratio for flakes was 2.22 (standard level of crosslinking). Crosslinking lasted for 16 hours. The crosslinked chitosan particles were extensively rinsed with demineralized water. This general procedure was applied to manufacture crosslinked chitosan flakes at four particle sizes: G1 < 125 µm < G2 < 250 µm < G3 < 500 µm < G4 < 710 µm. Dissolution testing in sulfuric acidic solutions (pH ca. 3) has shown that chitosan does not significantly dissolve after the crosslinking step: chitosan concentration in the

solution was measured using the acid red titration method [24]. These findings demonstrate that the crosslinking is stable in our experimental conditions. A pycnometer measurement of the density of the crosslinked flakes showed that the density is almost constant for each of the size fractions and crosslinking ratio. The mean value, calculated on nine samples, was found to be 1.36 kg L^{-1}.

Experimental Procedure for Palladium Sorption

Palladium solutions were prepared from palladium chloride ($PdCl_2$, ChemPur) in demineralized water (except in studies of the influence of chloride ions, which were added in the form of NaCl). Alternatively, for duplicate experiments, palladium solutions were prepared from ammonium tetrachloropalladate ($(NH_4)_2PdCl_4$, ChemPur), and experiments have confirmed that palladium is not influenced by the kind of palladium salt. The pH of the solutions was controlled using either hydrochloric acid or sulfuric acid, and sodium hydroxide concentrated solutions (5 M). The pH was kept constant during the sorption step with the exception of the studies on the optimization of the sorption pH.

For sorption isotherms, known volumes of palladium solutions (100 mL) at fixed concentration (10, 20 or 40 mg L^{-1}) were put in contact with varying sorbent quantities (ranging from 5 to 30 mg wet mass) at room temperature (20 °C ± 1 °C). After 3 days of agitation, in a reciprocal shaker, solutions were filtered through 1.2 µm filtration membranes and the filtrates were analyzed using the $SnCl_2$/HCl spectrophotometric method (using a SHIMADZU 1601 UV-Visible spectrophotometer, Japan) or alternatively using ICP analysis (JOBIN-YVON JY36, France) [25]. Control experiments showed that no sorption occurred on either glassware or filtration systems. The sorption capacity, or palladium concentration in the sorbent, was obtained using a mass balance equation, and was expressed as mg Pd g^{-1} sorbent, without reference to actual chitosan content in the sorbent which is in turn dependent on the crosslinking ratio.

For the study of sorption kinetics, a standard procedure was applied [11]. 1 L of palladium solution at fixed pH was mixed with either 50 mg or 150 mg of sorbent, in a jar-test agitated system (240 rotations per minute). 5 mL samples were withdrawn at specified times and filtered through a 1.2 µm filtration membrane and analyzed as previously specified. Alternatively, in selected experiments, the sorbent mass was varied to determine the influence of both the sorbent dosage and the crosslinking ratio.

For the study of sorption in continuous sytems, a column (internal diameter: 7 mm) was filled with differing amounts of sorbent and was fed with an acidic solution of palladium (pH 2) with different flow rates. Samples were regularly collected and analysed.

Empirical Modeling of Breakthrough Curves

The breakthrough curves were drawn as a function of the bed volumes (BV) passed through the column based on empty-bed column volume V_c,(m^{-3}), V_c= Z S, where Z is the column depth (m) and S the cross-section area of the column (m^2). The experimental data were mathematically matched to the following equation:

$$\frac{C(t)}{C_o} = \frac{1}{1 + \mathrm{Exp}\left[-\alpha\left(BV - BV_o\right)\right]} \qquad (1)$$

where BV_o and α are the parameters to be determined. They were determined using a nonlinear regression analysis (Levenberg-Marquardt algorithm included in the Mathematica® software). BV_o represents the virtual volume of the solution for which the outlet concentration reaches 50 % of the inlet concentration. Assuming the breakthrough curve being symmetrical around the point (BV_o,0.5) , BV_o could be theoretically correlated with the concentration of the sorbate C_o, the amount of sorbent in the volume V_c, m, and the sorption capacity $q(C_o)$ (determined from the sorption isotherms) corresponding to an equilibrium concentration equal to the inlet concentration according to:

$$BV_o\ C_o\ V_c = m\ q(C_o) \qquad (2)$$

Equation (1) may be transformed to:

$$BV = BV_o - \frac{1}{\alpha}\ln\left(\frac{C_o}{C(t)} - 1\right) = \frac{U_o\, t}{Z} = \frac{\upsilon\, \varepsilon\, t}{Z} \qquad (3)$$

where U_o is the superficial flow velocity (U_o = Q/S), Q is the flow rate ($m^3\ h^{-1}$), υ represents the linear flow velocity, or interstitial flow velocity (m h^{-1}), $\upsilon = U_o/\varepsilon$, ε is the column voidage (the column voidage with this flake shape of particules was found to vary between 0.73 and 0.79, the average value has been taken for calculations: 0.76), and Z the column depth (m).

This equation is similar to those derived from Bohart and Adams model [20] which gives:

$$t = \frac{N_o\, Z}{C_o\, \upsilon} - \frac{1}{k\, C_o}\ln\left(\frac{C_o}{C(t)} - 1\right) = s\, Z - s_o \qquad (4)$$

$$\ln\left(\frac{C_o}{C(t)} - 1\right) = \ln\left(\mathrm{Exp}\left[\frac{k\, N_o\, Z}{\upsilon}\right] - 1\right) - k\, C_o\, t \qquad (5)$$

where N_o is the volumetric sorption capacity (kg m^{-3}) and is equal to $q(C_o)(1-\varepsilon)\rho/\varepsilon$, where ρ represents the sorbent volumetric mass (kg m^{-3}) respectively. The kinetic constant is represented by k (m^3 kg^{-1} h^{-1}). The critical bed depth Z_o is obtained for t = 0 and for a fixed outlet concentration $C(t) = C_b$ (C_b is the concentration at the breakthrough defined as a limit concentration or a fixed percentage of the inlet concentration):

$$Z_o = \frac{\upsilon}{k N_o} \ln\left(\frac{C_o}{C(t)} - 1\right) = \frac{\upsilon}{k N_o} \ln\left(\frac{C_o}{C_b} - 1\right) \quad (6)$$

The critical bed depth represents the theoretical depth of sorbent necessary to prevent the sorbate concentration to exceed the limit concentration C_b. Another important parameter is the coefficient s_o defined using the Hutchins equation (derived from equation (4)) [22]. It represents the time required for the adsorption wave front to pass through the critical bed depth. It is obtained from:

$$s_o = \frac{1}{k C_o} \ln\left(\frac{C_o}{C_b} - 1\right) \quad (7)$$

The coefficient s, is the slope of equation (4), it represents the time required to exhaust a unit length of the column under the selected experimental conditions and with the limit outlet concentration:

$$s = \frac{N_o}{C_o \upsilon} \quad (8)$$

Results and Discussion

Palladium Sorption on Glutaraldehyde Crosslinked Chitosan: Isotherms and Kinetics in Batch Systems

Figure 1 presents palladium sorption isotherms for different particle sizes of sorbent at pH 2. Experimental data can be described by either the Langmuir equation or the Freundlich equation:

Langmuir equation
$$q = \frac{q_m b C_{eq}}{1 + b C_{eq}} \quad (9)$$

Freundlich equation
$$q = k_F C_{eq}^{1/n} \quad (10)$$

where q (mg g^{-1} or mmol g^{-1}) and C_{eq} (mg L^{-1} or mmol L^{-1}) represent the concentration at equilibrium in the solid and the liquid phases respectively; q_m is the maximum sorption capacity at saturation of the monolayer (mg g^{-1} or mmol g^{-1}), and b the ratio of sorption to desorption rates (L mg^{-1} or L $mmol^{-1}$). k_F ($mg^{1-1/n}$ g^{-1} $L^{-1/n}$) and n are the parameters of the Freundlich model.

Table 1 presents the values of the Langmuir and the Freundlich model parameters for palladium sorption on glutaraldehyde crosslinked chitosan for different particle sizes of sorbent. The MSR coefficient shows that the Freundlich model fits better the experimental data than the Langmuir equation.

Moreover, it is possible to see that the particle size hardly influences sorption isotherms: the sorption capacity is not influenced by the diameter of sorbent particles. This finding contrasts with previous results on the sorption of uranium using chitosan flakes [26], and the extraction of molybdate with crosslinked chitosan flakes [27]. In the latter cases, the diffusion of polynuclear ions of large ionic size is sterically hindered by the low porosity of chitosan, and sorption is restricted to the external layers of the biopolymer. A chitosan gel conditioning may reduce this hindering effect [11]. The weak effect of particle size on sorption capacities is an important characteristic for the design of fixed-bed systems: the volumetric capacity of the columns will only be changed by the change in the void fraction of the column when the particle size is increased.

Another important characteristic of these sorption isotherms appears in the shape of the curves: palladium sorption on glutraldehyde crosslinked chitosan is very favourable. Sorption capacity increases strongly at low residual concentration and reaches a quasi-plateau: sorption capacity will not be significantly changed above a 10 mg L^{-1} residual palladium concentration.

Figure 2 presents the influence of particle size on palladium sorption kinetics. Though increasing particle size increases the time required to reach equilibrium, the influence of this parameter is not very strong in comparison to the sorption of other metal anions (such as molybdate and vanadate) on similar sorbents [11]. The sorption of metal ions may be controlled by their diffusion in the polymer network. Chitosan being a low porous material, increasing the size of sorbent particle limits mass transfer of large molecules such as polynuclear hydrolysed molybdate, while the diffusion of mononuclear species such as hexachloroplatinate and tetrachloropalladate anions is hardly influenced [8]. Owing to the weak effect of particle size on sorption kinetics in batch systems, this parameter is suspected to hardly affect breakthrough curves, however particle size may influence external diffusion coefficient in fixed-bed column. Sorption kinetics are more significantly affected by metal concentration as shown on Figure 3. Increasing the initial concentration increases significantly the time required to reach equilibrium, the slope of the decay

curves decreases with large metal concentrations (Figure 3a). It may vary the depth of the sorption zone and then influences the slope of the breakthrough curves. However, Figure 3b shows that sorption rate (amount of palladium adsorbed on the solid) increases with the initial concentration.

Influence of Palladium Concentration on Breakthrough Curves

Figure 4a shows the influence of inlet palladium concentration on the breakthrough curves. As expected, increasing the metal concentration reduces the breakthrough volume significantly, however this reduction is not proportional to that of metal concentration: it seems that increasing the concentration makes the system more efficient. Figure 4b shows the same curves with a different x-axis (the volume -in bed volumes- time the initial concentration): it confirms that increasing metal concentration increases the amount of metal to be treated by the sorbent before the breakthrough. The difference is not so significant when the exhaustion points are compared (Figure 4b). Moreover, as expected, with increasing metal concentration, the slope of the breakthrough curves increases indicating a better mass transfer in the column. Palladium concentration at column exhaustion increases with the initial concentration reaching 150 mg g^{-1}, 178 mg g^{-1} and 198 mg g^{-1} for 5 mg L^{-1}, 25 mg L^{-1} and 50 mg L^{-1} respectively. These values are close to that obtained for sorption isotherms: 155 mg g^{-1}, 170 mg g^{-1} and 182 mg g^{-1} respectively. Table 2 shows the modeling of breakthrough curves with the empirical equation (1), the coefficient α increases with the concentration. This coefficient may be related to the slope of the breakthrough curve at the half exhaustion point ($C(t) = 0.5\ C_o$) according to:

$$\left[\frac{d\left(\frac{C(BV)}{C_o}\right)}{d\,BV}\right]_{BV=BV_o} = \frac{\alpha}{4} \qquad (11)$$

Table 2 confirms that the slope of the curve increases with the inlet concentration and the variation follows:

$$\alpha = 1.211\ 10^{-4}\ C_o^{1.349} \qquad (R^2: 0.989) \qquad (12)$$

Table 3 presents the standard Bohart and Adams - Hutchins coefficients of the BDST model calcualted from equations (4-8) and deduced from the modeling of breakthrough curves using equation (1). The kinetic parameter, k, does not vary continuously with the concentration. No

explanation has been found to this trend. As expected increasing the inlet concentration increases the volumetric capacity of the sorbent in the column from 62 g L^{-1} to 79 g L^{-1}. These values may be converted to sorption capacities using the apparent volumetric mass of the sorbent in the column and the mass of the used for the each experiment and dynamic sorption capacities ranges between 160 mg g^{-1} and 200 mg g^{-1}, values close to that obtained in batch systems. The volumetric capacity N_o varies almost linearly with the concentration following the equation:

$$N_o = 59.87 + 360.5\, C_o \qquad (R^2 = 0.976) \qquad (13)$$

The breakthrough time is defined as the time required to reach an outlet concentration representing 5 % of the inlet concentration, while the exhaustion is defined as the time when the outlet concentration reaches 95 % of the inlet concentration. The critical bed length of the column decreases when the concentration increases from 5 mg L^{-1} and 25 mg L^{-1}, after what it stabilizes. On the other hand, as expected, the time required to exhaust a unit length of the sorbent in the column (s) under the test conditions and the time required for the adsorption wave front to pass through the critical bed depth (s_o) varies with the reciprocal of the concentration.

Increasing metal concentration progressively increases the degree of sorbent usage (DoSU), defined as the ratio of the metal sorbed at the breakthrough to the metal adsorbed as the exhaustion of the column (Table 4). The sorbent usage rate (sorbent mass used at the breakthrough volume) varies linearly with the concentration, according the equation:

$$SUR = 33.11\ 10^{-3} + 5.308\, C_o \qquad (R^2 = 0.995) \qquad (14)$$

It allows to readily manage the change of column systems under experimental conditions corresponding to a constant feed concentration.

Influence of Superficial Flow Velocity on Breakthrough Curves

Figure 5 shows the effect of the superficial velocity on palladium sorption breakthrough curves. The influence of this parameter is almost negligible. Chase discuss the influence of the usual operating parameters on the shape of the breakthrough curves and observe that the flow velocity has no significant effect on the position and the shape of the curves when the the reciprocal of the coefficient b of the Langmuir equation is negligible in front of the inlet concentration [28]. Though the sorption isotherms is more accurately described by the Freundlich equation, we will use this

criterium to evaluate the influence of this parameter. The criterium proposed by Chase is satisfied here and the weak effect of flow velocity is explained.

The overlapping of breakthrough curves indicates that mass transfer in fixed-bed columns is not controlled by superficial velocity with the selected experimental conditions (in this velocity range). The slight variations may be more certainly due to experimental inaccuracies rather than to a difference in the mass transfer. The empty bed contact time (EBCT) is given in Table 4 and for this experimental series, the EBCT varies between 1.7 and 7.3 min. Taking into account the voidage of the column (ε : 0.76) the mean residence time varies between 1.3 and 5.6 min. In spite of a so short residence time, the sorption is very efficient and weakly affected by flow velocity. This result may be related to the fast sorption kinetics obtained in batch systems (Figures 2 and 3): sorption rates are significantly higher than those observed with molybdate for example. Consequently palladium sorption breakthrough curves are less affected by flow rate in the column than were those for molybdate using similar sorbents [29-30].

BV_o and α is almost unchanged with increasing superficial flow velocity (Table 2): the variation does not exceed 5 %. The coefficient α slightly increases with decreasing the flow velocity. However, the slope of the linear part of the breakthrough curves is not so strongly affected by flow velocity, as it was for molybdate sorption [29-30]. The sorption capacity varies but in the same order of magnitude. This finding is consistent with the conclusions of a previous study of McKay et al. on dye binding using chitin in dynamic systems [31]. Kast and Otten have shown that in the case of a favourable isotherm (concave isotherm such as encountered with Langmuir-type isotherms) the slope of the curve becomes progressively steeper as the favorability of the isotherm increases [32]. In the case of palladium sorption, the Freundlich equation fits well experimental sorption isotherm and the sorption is very favourable (steep curve at low residual concentrations). The kinetic coefficient varies with the superficial flow velocity according to the equation:

$$k = 7.37\ 10^{-3} + 6.003\ U_o \qquad (R^2 = 0.999) \qquad (15)$$

The kinetic coefficient, k, depends on the effect of both external and intraparticle diffusion [23]. While the external diffusion is controlled by the flow velocity (this control may be predicted using well-knwon correlations such as that proposed by Williamson, [33]), intraparticle diffusion is not affected by flow rate. The dependence of the rate parameter with flow velocity indicates that both

mechanisms are rate controlling [23]. The occurence of several intraparticle diffusion mechanisms, including pore and surface diffusion makes the discussion of the influence of diffusion mechanisms on the shape of the breakthrough curves very difficult. Ma et al. [34] have concluded that the shape of the curve depends on the predominence of pore or surface diffusion which, in turn, depends on both the type of sorption isotherm which describes the equilibrium and the solute concentration.

The SUR and the DoSU do not significantly change with the superficial velocity under selected experimental conditions: SUR varies between 0.294 kg m^{-3} and 0.315 kg m^{-3} and the DoSU is in the range 82-83 %. It makes the fixed-bed system easy to manage: the change of the exhausted column may readily be predicted.

Influence of Column Depth (Sorbent Amount) on Breakthrough Curves

Increasing the column depth is expected to affect the volume of solution corresponding to an outlet concentration of 50 % of the inlet concentration [23], however reporting the breakthrough curves as a function of the bed volume allows the influence of the geometry of the column to be reduced and similar breakthrough curves would be expected. The bed volume of solution for half exhaustion (C_s/C_o = 0.5) would be expected to be almost identical for different amounts of sorbents (and different column depth), while the slope of the breakthrough curves would change with column depth: increasing the depth of the column increases the contact time between the sorbent and the sorbate. In the case of low porous sorbents for which the intraparticle diffusion is the rate limiting step, it would strongly affect breakthrough curves. In the case of palladium uptake, the sorption process is considered to be less affected by intraparticle diffusion than that of large polynuclear hydrolysed species (case of molybdate). In this study, palladium diffusion is not really sterically hindered. For differing column depths (2.4 cm, 4.5 cm and 6.6 cm), the sorption capacity at exhaustion are comparable (from 195 mg g^{-1} to 199 mg g^{-1}). However for short column, the breakthrough occurs at a lower bed volume number and the slope of the curve is reduced: increasing column depth increases the EBCT from 2 to 6 min and the residence time from 1.5 to 4.6 min. The differences are not very marked, certainly as a consequence of the very efficient mass transfer of palladium in sorbent flakes. This result contrasts with the strong effect of column depth on breakthrough curves obtained for uranium sorption using chitosan flakes [35]: in the case of uranium sorption, intraparticle diffusion is considered a limiting step in the sorption process.

Increasing the depth of the column involves small variations of the parameters of the models (Tables 2-4): No, BVo and a slightly increase, while k, DoSU and SUR slightly decrease. However the variations are significantly lower than in changing the flow velocity and the inlet concentration of palladium. The most significant differences are observed for the shortest column size. The critical bed depth progressively increases with the depth of the column, however Z_o represents a decreasing fraction of the total column depth with increasing this parameter: 22 %, 19 % and 15 % for 2.4 cm, 4.5 cm and 6.6 cm-long columns respectively.

Influence of Column Diameter on Breakthrough Curves

Experiments were performed with differing column diameter (Figure 7). The figure shows 3 breakthrough curves obtained with the same column depth (10 mm - 2.3 cm, and 7 mm - 2.4 cm) and with the same amount of sorbent (10 mm - 2.3 cm, and 7 mm - 4.5 cm) with the same superficial flow velocity. The comparison of these 3 curves allows to detect and separate the respective influence of column depth and column diameter. The change in the column diameter does not change the breakthrough curves (neither BV_o nor α) for similar column depth. For comparable sorbent amounts (10 mm - 2.3 cm, and 7 mm - 4.5 cm), the lowest column depth used for the experiment with column diameter 10 mm is less favourable to sorption, perhaps due to a too short contact time and to dispersion effects.

This finding is consistent with previous results on the effect of column depth (Figure 6). For the same amount of sorbent, enlarging the column results in a diminution of both column depth and residence time. As a consequence, the resistance to diffusion may limit the overall mass transfer and the sorption efficiency.

Influence of Sorbent Particle Size on Breakthrough Curves

Kast and Otten have shown that in the case of a favourable isotherm (concave isotherm such as encountered with Langmuir-type isotherms) the slope of the curve becomes progressively steeper as the favorability of the isotherm increases [23]. In the case of palladium sorption, the Freundlich equation fits well experimental sorption isotherm and the sorption is very favorable (steep curve at low residual concentrations). Sorption isotherms are not really affected by sorbent particle size and the curves are overlapped. In these conditions, this experimental parameter is assumed to be non-

limiting. Surprisingly, Figure 8 shows that increasing the size of sorbent particles reduces sorption performance (greater volume at breakthrough and at exhaustion of the column). One would expect a reciprocal trend: increasing the sorbent particle size usually limits mass transfer. No explanation of this experimental which was obtained several times have yet been found. The figure presents breakthrough curves for G2 and G3 particles with their actual depth in the 7 mm-diameter columns for a sorbent mass of 0.5 g (4.5 cm for G2-fraction and 6.7 cm for the G3-fraction). The voidage fraction in the column increases with the size of the sorbent flakes from 76 % to 86 % for G2 and G3 fractions respectively. This finding could explain this unexpected trend.

Sorption capacity is also increased. These results contrast with those from sorption isotherms in batch systems. Sorbent particle size may influence sorption kinetics (Figure 2) but not equilibrium. In these conditions we could expect a similar 50 % breakthrough point (comparable BV_o), but a lower breakthrough slope. A reverse trend is observed on experimental data: breakthrough slopes are comparable while the breakthrough volume at 50 % of the inlet concentration is significantly decreased for largest particles. Surprisingly, using the G3 size fraction leads to a higher DoSU, a lower SUR, compared to G2 fraction (Table 4). The kinetic coefficient k, and the time required for the adsorption zone to pass through the critical bed depth are not significantly affected by the size of the particle (Table 3). The critical bed depth is increased by 15 % but it represents only 16 % of the total depth of the column. As expected, increasing the size of the sorbent induces a strong decrease of the volumetric sorption capacity, however the variation is not proportional to the volume variation of the column (V_c). The time required to exhaust a unit length of the sorbent is also strongly decreased. Ko et al. have studied the effect of particle size on breakthrough curves for metal ion sorption on bone char sorbents [23]. They attribute the increase in sorption performance with decreasing the size of the sorbent particles to diffusion restrictions. They underline the effect of increasing the particle size on the increase of the column depth to partly explain these results. The discrepancies between experimental data and predictions from Hutchins and Bohart-Adams model has been also attributed to the fact that the basic hypothesis of these models is not verified in these systems (ca. a rectangular sorption isotherms) [23]. The influence of this parameter is not restricted to diffusion properties. It may affect the pressure drop inside the column, which can be calculated using the Ergun equation:

$$\frac{dP}{dZ} = \frac{\upsilon (1 - \varepsilon)}{d_p \varepsilon^3} \left(\frac{150 (1 - \varepsilon) \mu}{d_p} + 1.75 \rho_l \upsilon \right) \quad (16)$$

where μ and ρ_l are the viscosity (N s m^{-2}) and the volumetric mass of the solution (kg m^{-3}). Increasing the particle size of the sorbent may increase strongly the pressure drop in the column. The optimization of the process should take into account both hydraulic and mass transfer properties, and it seems preferible to avoid using the smallest size fraction (G1: 0.125 µm). The permeability coefficient was shown to vary between 1.4 10^{-12} m^2 and 17 10^{-12} m^2 under comparable experimental conditions [35]. In the case of uranium sorption, the influence of particle size on kinetics in both batch and columns systems was more marked, due to intraparticle diffusion limitations [26,35].

Influence of Competitor Ions on Breakthrough Curves

The presence of competitor anions involves a strong decrease in palladium sorption performances [7]. The sorption mechanism is assumed to be a ion exchange process involving the exchange of counter ion near the protonated amine groups or the electrostatic attraction of metal anions to these protonated amine groups. The presence of competitor anions reduces the number of amine groups available for palladium sorption. Figure 9 shows the breakthrough curves for palladium sorption on glutaraldehyde crosslinked chitosan flakes at pH 2, in presence of chloride, nitrate and sulfate anions, using standard experimental conditions: inlet concentration 50 mg L^{-1}; sorbent mass: 0.5 g; column depth: 4.5 cm, superficial flow velocity: 0.65 m h^{-1}. The influence of these anions is very strong but depends on the kind of anions.

Considering the volume at 50 % of the exhaustion (BV_o) he competitor effect may be clearly classified following the sequence: sulfate >> chloride > nitrate. Similar observations on the influence of competitor anions have been cited for platinum sorption using glutaraldehyde crosslinked chitosan [8]. It is interesting to note that in spite of nitrate concentration which is twice that of chloride, palladium sorption breakthrough curve in presence of nitrate is more favourable than that of chloride. The sulfate interaction is significantly stronger than that of chloride. This effect has been correlated to their differences in ionic radius, ionic charge and also to the different behaviour of these ions in presence of palladium: palladium may react with chloride to form anionic

species which are adsorbable, while sulfate anions do not interact with palladium. The speciation of palladium strongly depends on ph, total metal concentration and chloride concentration: in presence of sulfate anions instead of chloride anions (brought by sulfuric acid rather than hydrochloric acid for pH control) chloride concentration is not sufficient to form a number of adsorbable palladium species and the sorption efficiency decreases. To avoid such interferences or decrease their influence of platinum/palladium sorption, chitosan has been modified by grafting new functional groups including sulfur moities (thiourea, rubeanic acid) [16].

The slope of the breakthrough curves is similar for each curves with the exception of that obtained in presence of nitrate: in this case, the slope is steeper. The sorption capacity is greater but the mass transfer is more affected by the presence of nitrate. It is difficult to find an explanation to this result.

The presence of competitor ions involves a significant variation of model parameters (Table 2-4): (a) the critical bed depth, Z_o, and the sorbent usage rate, SUR, are significantly increased; (b) the volumetric capacity, N_o, the degree of sorbent usage at breakthrough, DoSU, and the time required to exhaust a unit of length of sorbent, s, are decreased; the kinetic coefficient, k, and the time required for the adsorption zone to pass through the critical bed depth, s_o, remains in the same order of magnitude. The presence of competitor ions mainly affects equilibrium parameters than kinetic parameters.

It is important to observe that sorption performances in the dynamic systems investigated in this study are mainly controlled by the presence of competitor ions than by the parameters related mass transfer (diffusion and hydraulic). This finding may be explained by the relative fast mass transfer of chloropalladate species in these sorbents in comparison to other metal-chitosan systems for which the control of mass transfer by diffusion properties let the hydraulic parameters control the sorption breakthrough curves owing to their influence on residence time and consequently on mass transfer resistance in columns.

Conclusion

Glutaraldehyde crosslinked chitosan flakes are very efficient at removing palladium from dilute solutions. Sorption capacities a high as 190-200 mg g^{-1}, have been obtained in batch systems. The same sorption levels are reached with fixed-bed column systems. Owing the relative fast sorption

kinetics obtained in palladium sorption with these sorbents (in batch systems), it is not suprising to obtain favourable sorption breakthrough curves: the curves are characterized by steep slopes.

The breakthrough curves are controlled by several experimental parameters such as the column depth, the superficial flow velocity, the metal concentration but also the size of sorbent particles. However though the effect of these parameters can not be neglected, the differences are not so marked as with other sorbent/sorbate systems. In the case of molybdate sorption, using chitosan gel beads, the influence of intraparticle diffusion on kinetic control is more marked and the breakthrough curves are more senstive to the variation in hydrodynamic parameters (flow velocity, column depth ...) and sorbent parameters (particle size, conditioning ...). In the case of palladium, the ready diffusion of mononuclear metal species is not sterically hindered as with systems involving the diffusion of polynuclear hydrolysed species (molybdate, vanadate ...).

The influence of competitor anions is more significant: a strond reduction in the volume of the solution which can be recovered with a unit of charge of sorbent is significantly reduced: a 0.1 molar solution of sulfate is sufficient to reduce the half exhaustion volume (BV_o) from 1150-1200 BV to 450 BV. This competitor effect may be significantly decreased by using modified chitosan obtained by grafting of sulfur derivatives on chitosan backbone: this modification of chitosan changes the anion exchange resin into a chelating resin, less sensitive to ionic strength, and to the presence of competitor anions.

References

(1) C.S. Brooks, *Metal Recovery from Industrial Wastes*, Lewis publishers, Chelsea, Michigan, 1991.

(2) Beauvais, R.A., Alexandratos, S.D. Polymer-Supported Reagents for the Selective Complexation of Metal Ions: an Overview. *React. Funct. Polym.*, **1998**, *36*, 113-123.

(3) Cortina, J.L., Miralles, N., Aguilar, M. Sastre, A.M. Distribution Studies of Zn(II), Cu(II) and Cd(II) with Levextrel Resins Containing Di(2,4,4-trimethylpentyl)phosphinic acid (Lewatit TP807'84), *Hydrometallurgy*, **1996**, *40*, 195-206.

(4) Fu, J., Nakamura, S., Akiba, K. Separation of Precious Metals through a Trioctylamine Liquid Membrane. *Sep. Sci. Technol.*, **1997**, *32*, 1433-1445.

(5) Fontas, C., Salvado, V., Hidalgo, M. Solvent Extraction of Pt(IV) by Aliquat 336 and its Application to a Solid Supported Liquid Membrane System, *Solvant Extr. Ion Exch.*, **1999**, *17* (1) 149-162.

(6) Remoudaki, E., Tsezos, M., Hatzikioseyian, A., Karakoussis, V., Mechanism of Palladium Biosorption by Microbial Biomass. The Effects of Metal Ionic Speciation and Solution Co-Ions, in: *Biohydrometallurgy and The Environment Toward the Mining of the 21st Century*, R. Amils and A. Ballester eds., Elsevier, Amsterdam, The Netherlands, Part B., 449-462, 1999.

(7) Ruiz, M., Sastre, A. and Guibal, E. Palladium Sorption on Glutaraldehyde-Crosslinked Chitosan. Submitted for publication in *React. Funct. Polym.*, 2000.

(8) Guibal, E., Larkin, A., Vincent, T., Tobin, J. Chitosan Sorbents for Platinum Recovery from Dilute Effluents. *Ind. Eng. Chem. Res.*, **1999**, *38* (10) 4011-4022.

(9) Kawamura, Y., Mitsuhashi, M., Tanibe, H., Yoshida, H. Adsorption of Metal Ions on Polyaminated Highly Porous Chitosan Chelating Resin. *Ind. Eng. Chem. Res.*, **1993**, *32*, 386-391.

(10) Piron, E., Accominotti, M., Domard, A. Interaction between Chitosan and Uranyl ions. Role of Physical and Physicochemical parameters on the Kinetics of Sorption. *Langmuir*, **1997**, *13*, 1653-1658.

(11) Guibal, E., Milot, C., Tobin, J.M. Metal-Anion Sorption by Chitosan Beads: Equilibrium and Kinetic Studies. *Ind. Eng. Chem. Res.*, **1998**, *37*, 1454-1463.

(12) Juang, R.-S., Ju, C.-Y. Kinetics of Sorption of Cu(II)-Ethylenediaminetetraacetic Acid Chelated Anions onto Cross-linked, Polyaminated Chitosan Beads. *Ind. Eng. Chem. Res.*, **1998**, **37**, 3463-3469.

(13) Baba, Y., Hirakawa, H. Selective Adsorption of Palladium(II), Platinum (IV) and Mercury (II) on a New Chitosan Derivative Possessing Pyridyl Group. *Chem. Lett.*, **1992**, 1905-1908.

(14) Inoue, K., Yamaguchi, T., Iwasaki, M., Ohto, K., Yoshizuka, K. Adsorption of Some Platinum Group Metals on Some Complexane Types of Chemically Modified Chitosan. *Sep. Sci. Technol.*, **1995**, *30*, 2477-2489.

(15) Wan Ngah, W.S., Liang, K.H. Adsorption of Gold(III) Ions onto Chitosan and N-Carboxymethyl Chitosan: Equilibrium studies. *Ind. Eng. Chem. Res.*, **1999**, *38*, 1411-1414.

(16) Guibal, E., Vincent, T., Navarro-Mendoza, R. Synthesis and Characterization of a Thiourea-Derivative of Chitosan for Platinum Recovery. *J. Appl. Polym. Sci.*, **2000**, 75, 119-134.

(17) Hsien, T.Y., Rorrer, G.L. Heterogeneous Cross-linking of Chitosan Gel Beads: Kinetics, Modeling and Influence on Cadmium Ion Adsorption Capacity. *Ind. Eng. Chem. Res.*, **1997**, *36*, 3631-3638.

(18) Tien, C. *Adsorption Calculations and Modeling*. Butterworth-Heinemann, Boston, 1994.

(19) Fernandez, M.A., Laughinghouse, W.S., Carta, G. Characterization of Protein Adsorption by Composite Silica-Polyacrylamide Gel Anion Exchangers II. Mass Transfer in Packed Columns and Predictability of Breakthrough Behavior, *J. Chromatogr. A*, **1996**, *746*, 185-198.

(20) Kawamura, Y., Yoshida, H., Asai, S., Tanibe, H. Breakthrough Curve for Adsorption of Mercury (II) on Polyaminated Highly Porous Chitosan Beads. *Wat. Sci. Technol.*, **1997**, *35*(7) 97-105.

(21) Bohart, G.S., Adams, E.G. Some Aspects of the Behaviour of Charcoal with Respect to Chlorine, *J. Chem. Soc.*, **1920**, *42*, 523.

(22) Hutchins R.A. New Method Simplifies Design of Activated Carbon Systems, *Chem. Eng.*, **1973**, *Aug.*, 133-138.

(23) Ko, D.C.K., Porter, J.F., McKay, G. Correlation-Based Approach to the Optimization of Fixed-Bed Sorption Units. *Ind. Eng. Chem. Res.*, **1999**, *38*, 4868-4877.

(24) Roberts, G.A.F. *Chitin Chemistry*. MacMillan, London, 1992.

(25) Charlot, G. *Dosages Absorptiométriques des Eléments Minéraux.* Masson ed., Paris, 1978.

(26) Guibal, E., Jansson-Charrier, M., Saucedo, I., Le Cloirec, P. Enhancement of Metal Ion Sorption Performances of Chitosan: Effect of the Structure on the Diffusion Properties, *Langmuir*, **1995**, *11*(2) 591-598.

(27) Milot, C., McBrien, J., Allen, S., Guibal, E. Influence of Physicochemical and Structural Characteristics of Chitosan Flakes on Molybdate Sorption, *J. Appl. Polym. Sci.*, **1998**, *68*, 571-580.

.

(28) Chase, H.A. Prediction of the Performance of Preparative Affinity Chromatography, *J. Chromatogr. A*, **1984**, *297*, 179-202.

(29) Milot, C. Adsorption de Molybdate(VI) sur Billes de Gel de Chitosane - Application au Traitement d'Effluents Molybdifères, Ph.D. Thesis, Université de Montpellier II, U.S.T.L. (France) 1998.

(30) Guibal, E., Milot, C., Roussy, J. Molybdate Sorption by Cross-Linked Chitosan Beads: Dynamic Studies,*Wat. Environ. Res.* , **1999**, *71*(11) 10-17.

(31) McKay, G., Blair, H.S., Gardner, J.R., The Adsorption of Dyes onto Chitin in Fixed Bed Columns and Batch Adsorbers, *J. Appl. Polym. Sci.*, **1984**, *29*, 1499-1514.

(32) Kast, W., Otten, W. The Breakthrough in Fixed Bed Adsorbers: Methods of Calculation and the Effects of Process Parameters. *Int. Chem. Eng.*, **1989**, *29* (2) 197-211.

(33) Weber, W.J., jr., DiGiano, F.A. *Process Dynamics in Environmental Systems*. Wiley & Sons, NY, 1996.

(34) Ma, Z., Whitley, R.D., Wang, N.-H. L., Pore and Surface Diffusion in Multicomponent Adsorption and Liquid Chromatography Systems, *AIChE J.*, **1996**, *42*(5) 1244-1262.

(35) Jansson-Charrier, M., Guibal, E., Roussy, J., Surjous, R., Le Cloirec, P. Dynamic Removal of Uranium by Chitosan: Influence of Operating Parameters, *Wat. Sci. Technol.*, **1996**, *34* (10) 169-177.

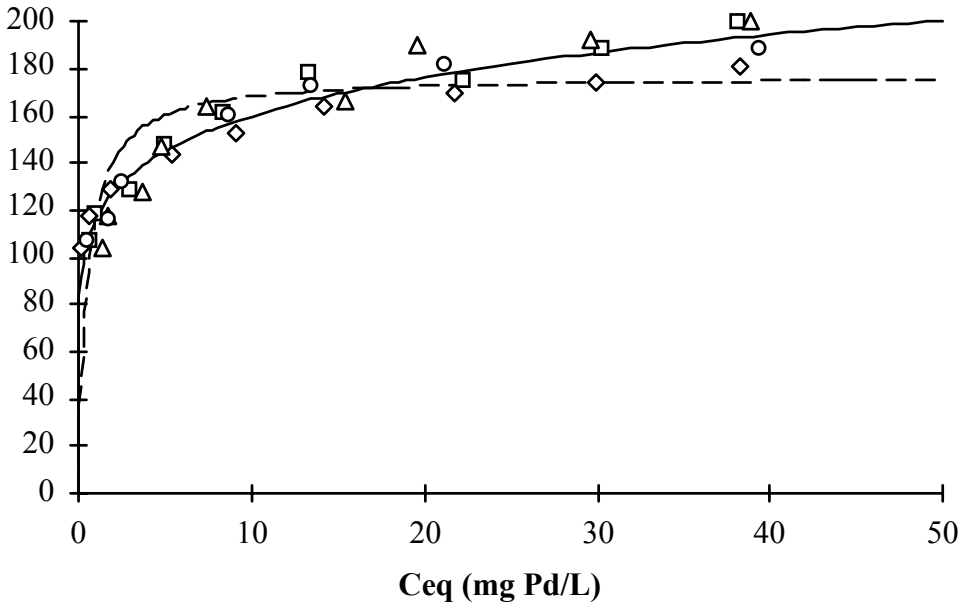

Figure 1: Influence of particle size on palladium sorption isotherms at pH 2 (pH controlled with HCl, G1: a; G2: ◊; G3: d; G4: O; solid line: Freundlich model, dashed line: Langmuir model for joined series).

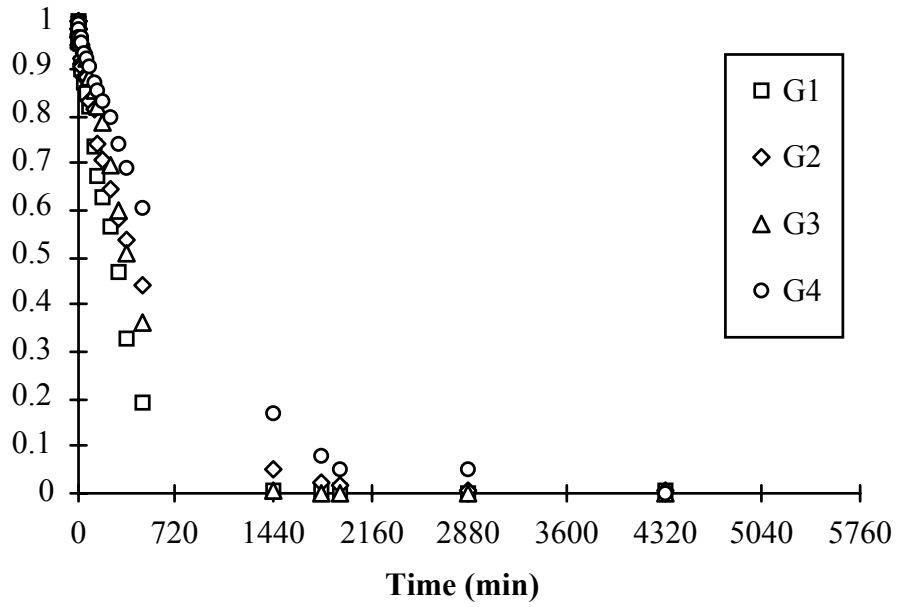

Figure 2: Influence of sorbent particle size (a: G1; ◊: G2; d: G3; o: G4) on palladium sorption kinetics at pH 2 (controlled with HCl; C_o: 20 mg Pd L^{-1}; SD: 100 mg L^{-1}).

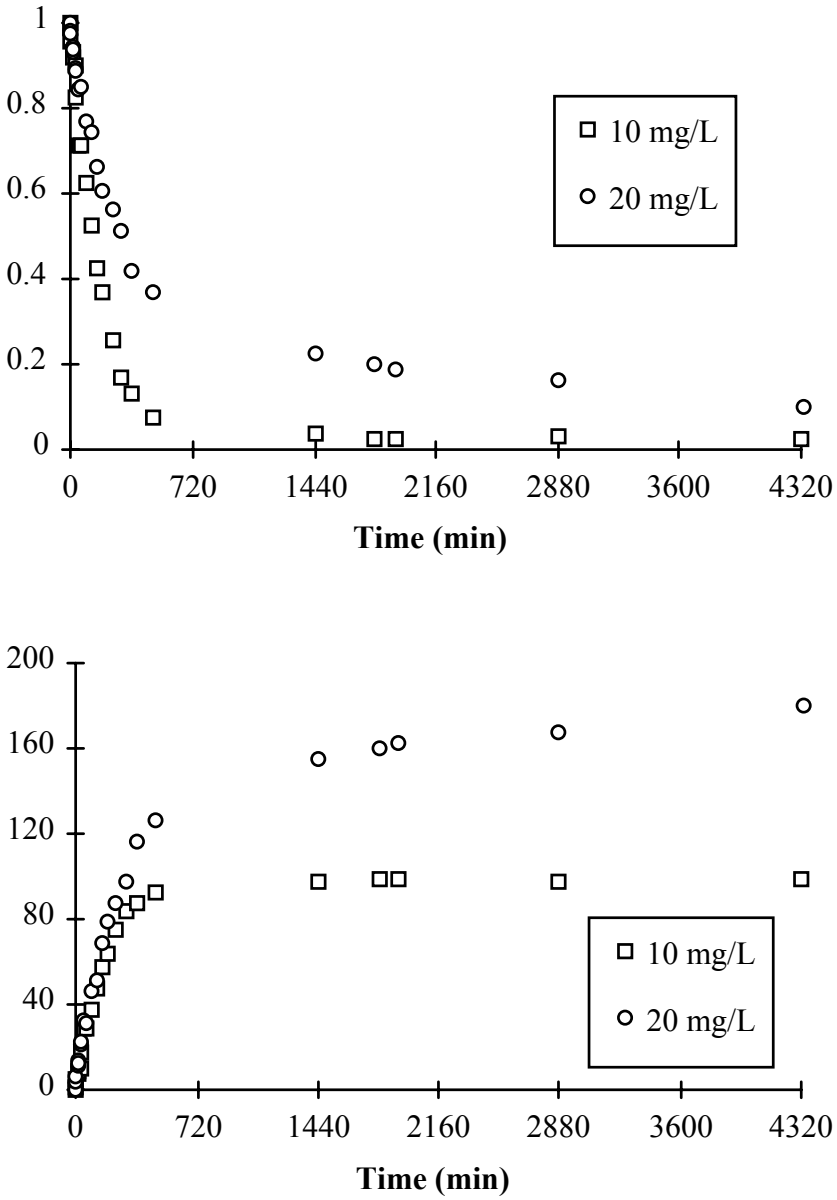

Figure 3: Influence of palladium concentration on sorption kinetics at pH 2 (controlled with hydrochloric acid; SD: 100 mg L^{-1}).

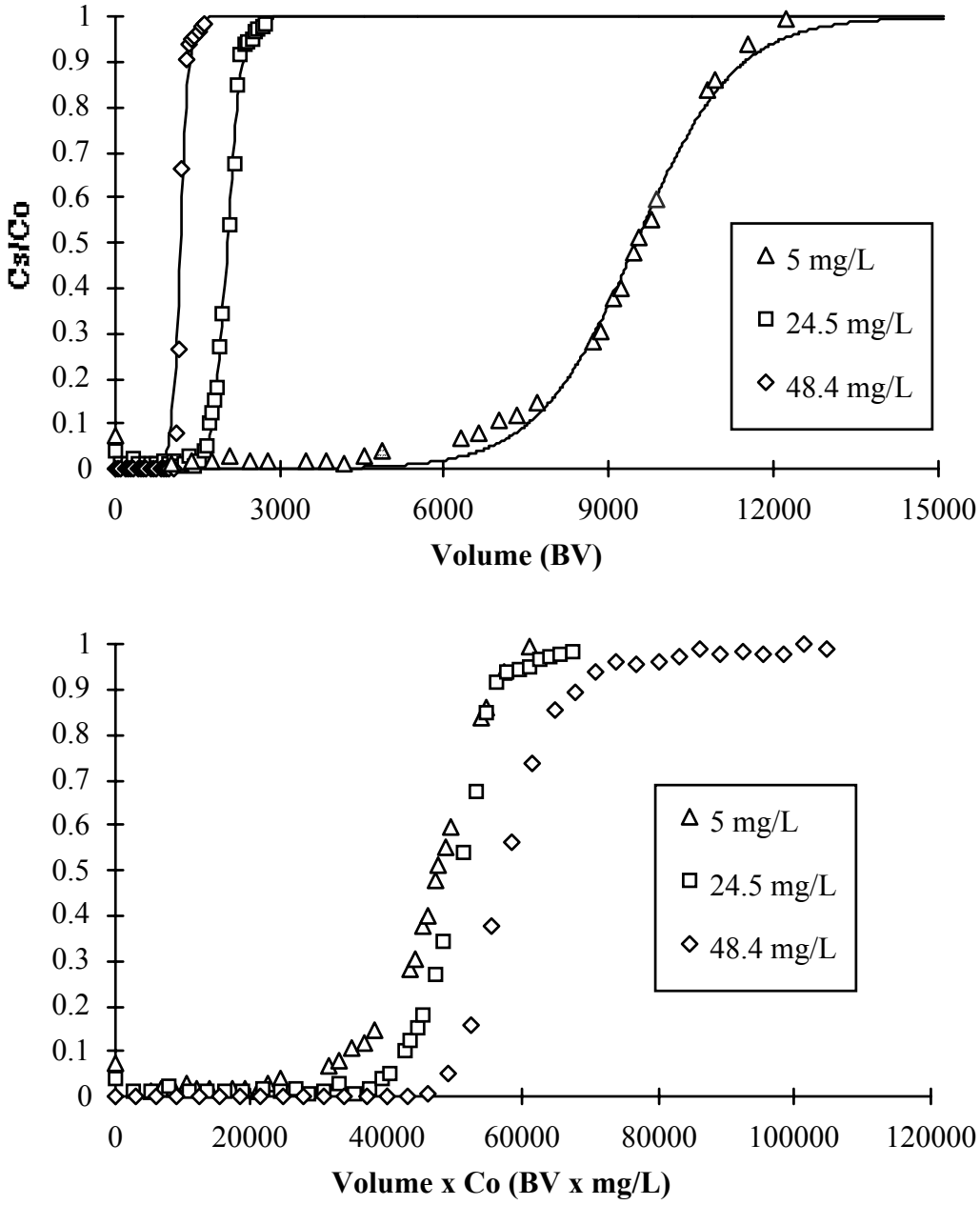

Figure 4: Influence of initial concentration on palladium sorption breakthrough curves.

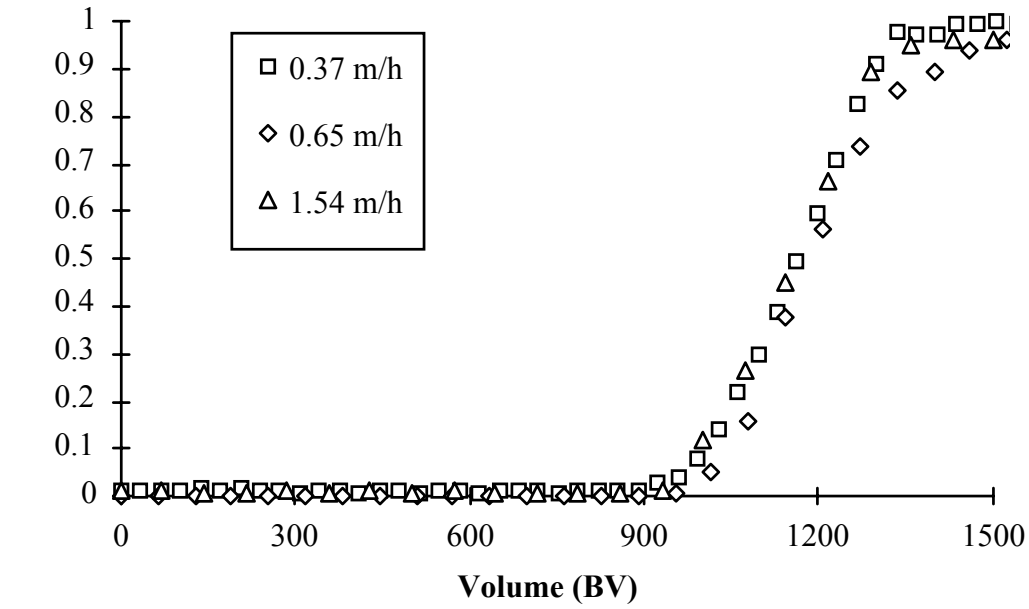

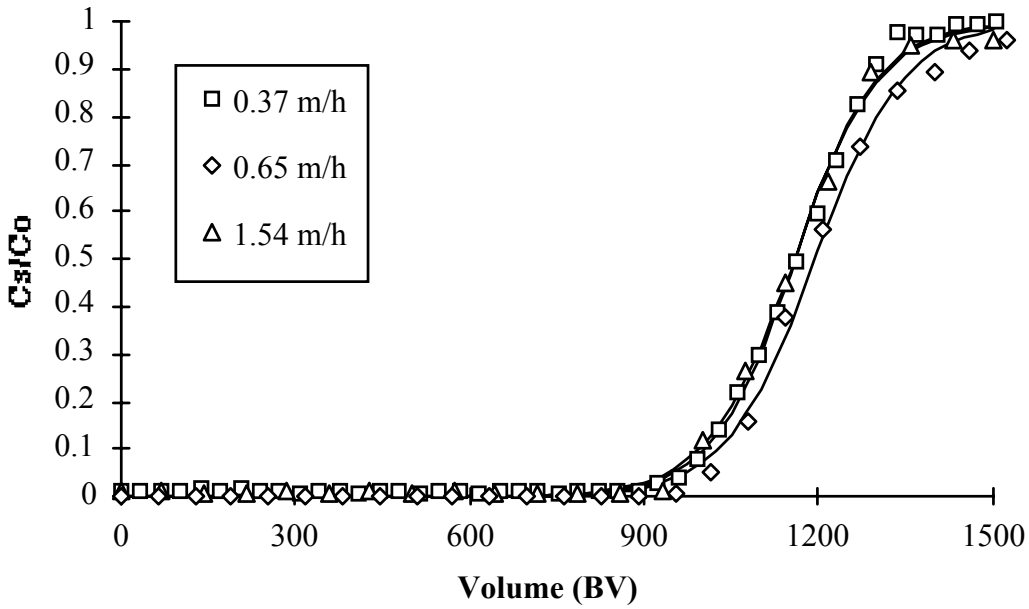

Figure 5: Influence of superficial velocity on palladium sorption breakthrough curves

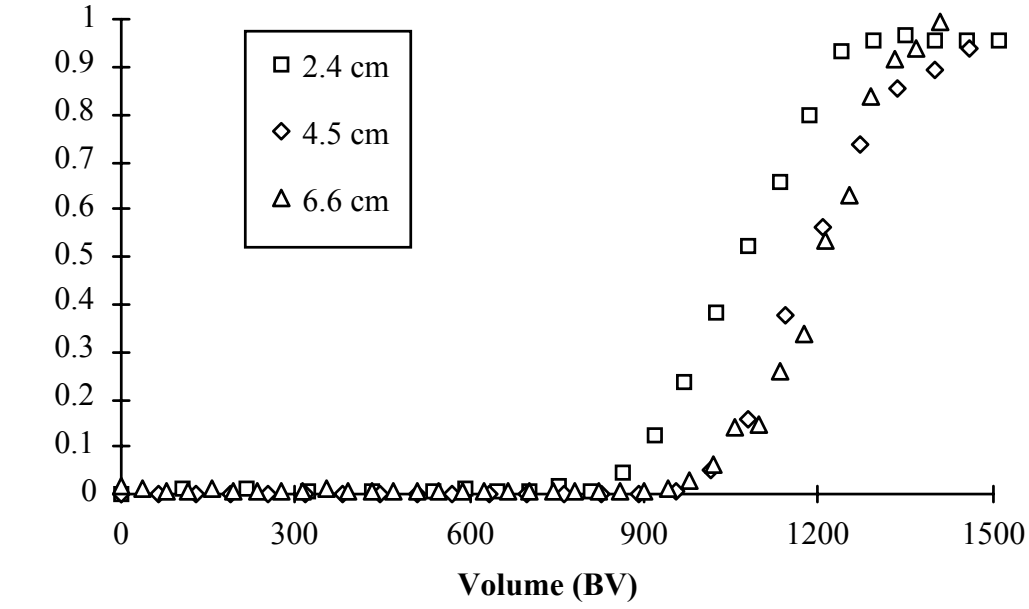

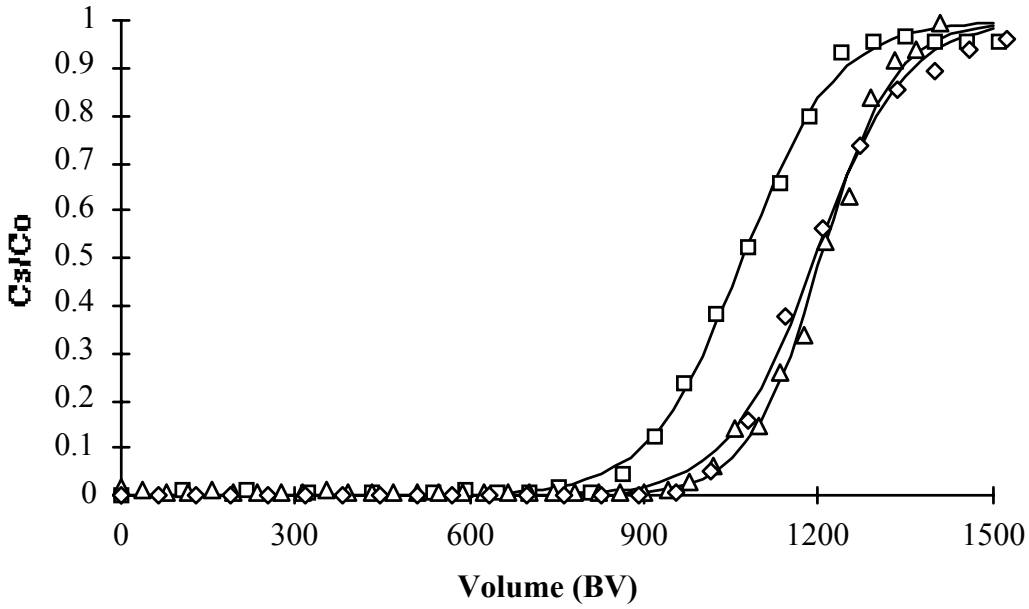

Figure 6: Influence of column depth on palladium sorption breakthrough curves.

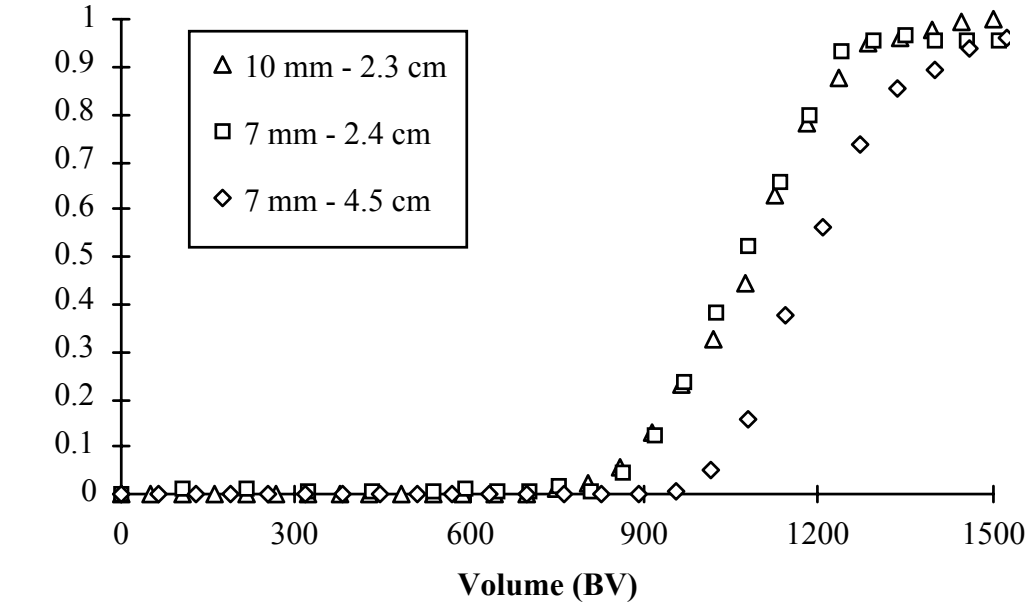

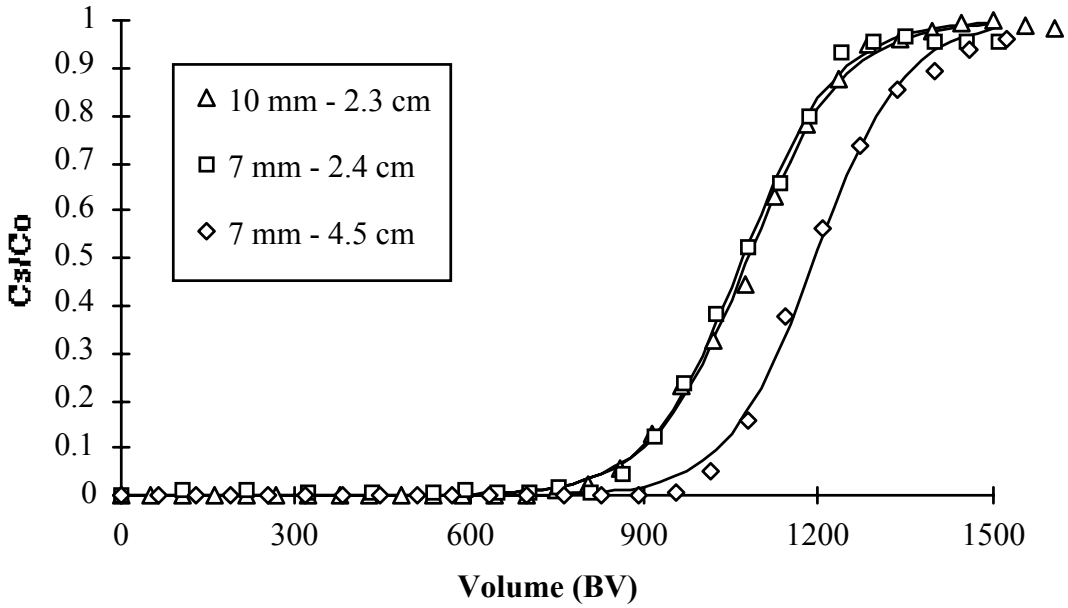

Figure 7: Influence of column diameter on palladium sorption breakthrough curves

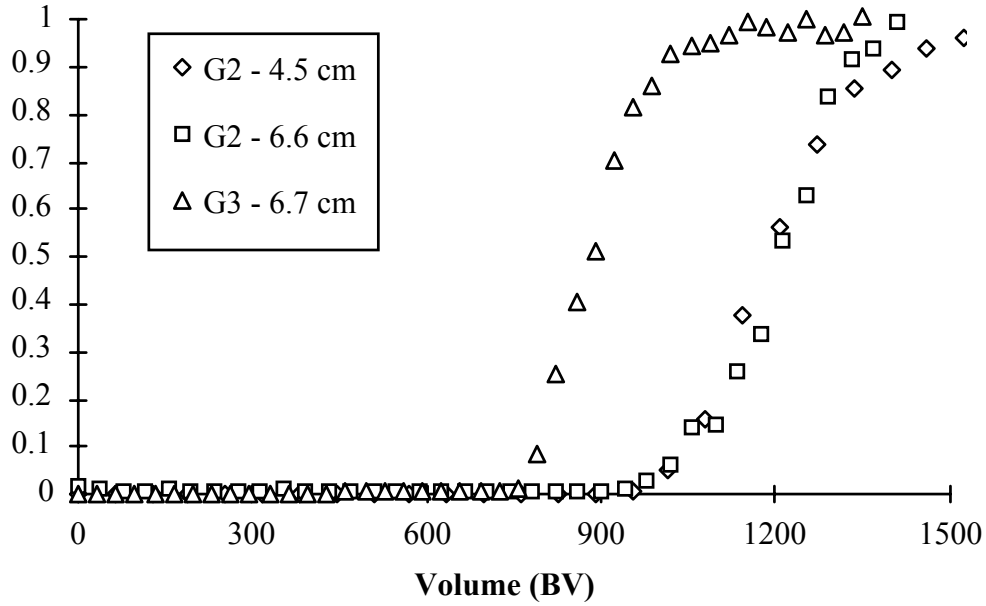
1
0.9
0.8
0.7
0.6
0.5
0.4
0.3
0.2
0.1
0
G2 - 4.5 cm
G2 - 6.6 cm
G3 - 6.7 cm
0
300
600
900
1200
1500
Volume (BV)

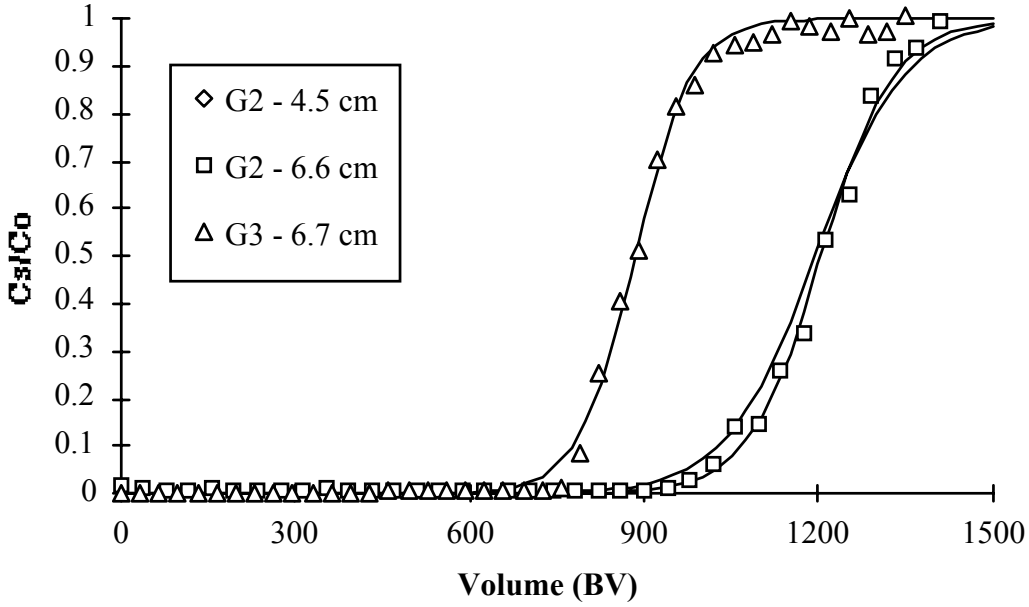
1
0.9
0.8
0.7
0.6
0.5
0.4
0.3
0.2
0.1
0
C/Co
G2 - 4.5 cm
G2 - 6.6 cm
G3 - 6.7 cm
0
300
600
900
1200
1500
Volume (BV)

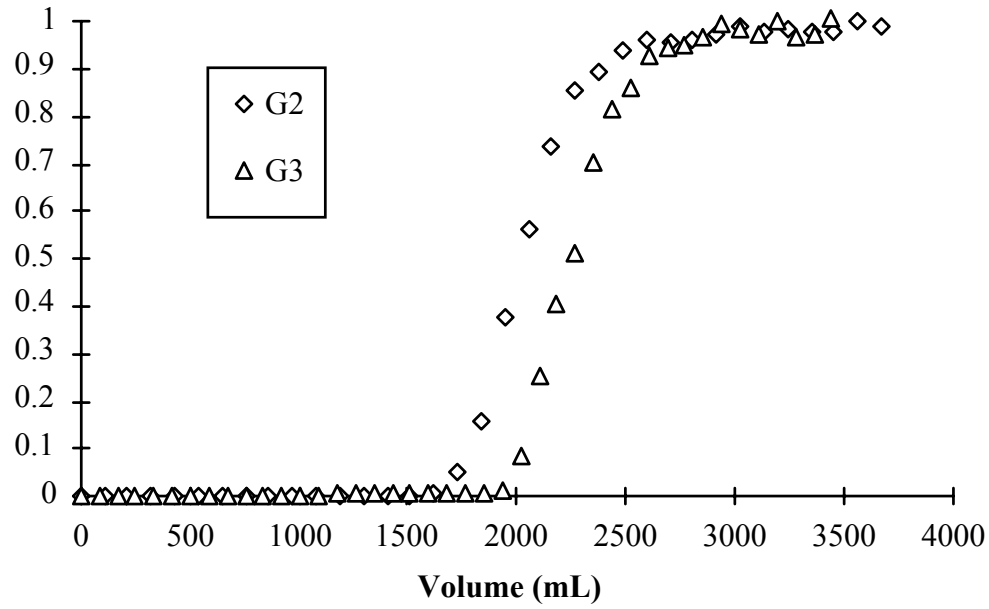

Figure 8: Influence of sorbent particle size on palladium sorption breakthrough curves

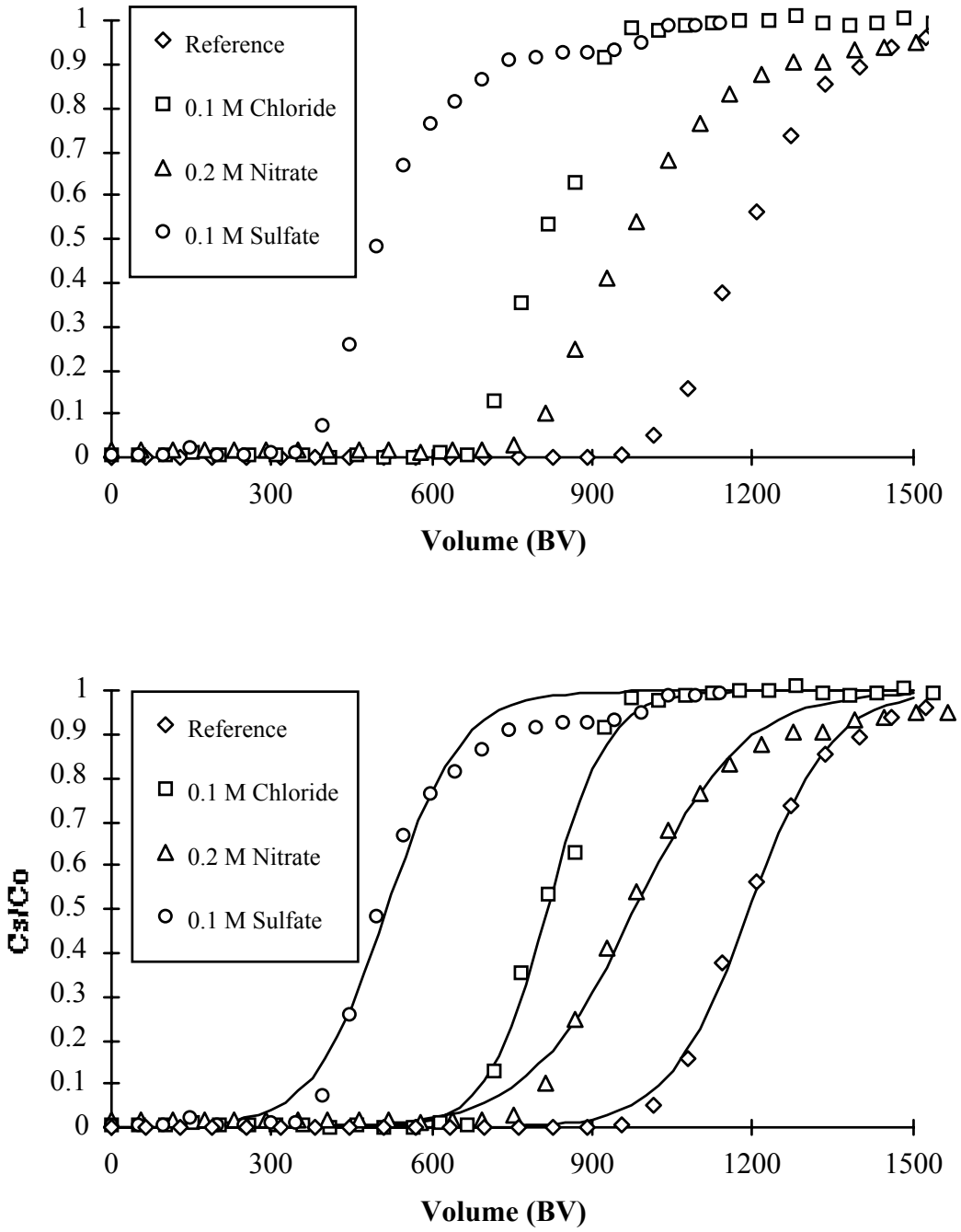

Figure 9: Influence of competitor ions on palladium sorption breakthrough curves

Table 1: Parameters of the Langmuir and Freundlich models for palladium sorption using glutaraldehyde-crosslinked chitosan with varying particle size at pH 2 (pH controlled with HCl)

	Langmuir model			Freundlich model		
Particle size	q_m (mg g^{-1})	b (L mg^{-1})	MSR	k ($mg^{1-1/n}$ g^{-1} $L^{-1/n}$)	n	MSR
G1	181.31	1.857	13.72	117.10	6.984	5.18
G2	162.64	5.594	11.04	122.07	9.756	4.17
G3	196.92	0.701	9.11	105.86	5.553	6.96
G4	179.68	1.664	13.02	114.95	6.900	4.81
Joined Series	177.05	1.902	16.57	115.62	7.094	7.51

MSR: Mean Sum Residuals according to:

$$MSR = \sqrt{\frac{\sum_{i=1}^{n}\left(F_{exp.}(C_i) - F_{calc.}(C_i)\right)^2}{n}}$$

with F is the function representative of the sorption equation (Langmuir or Freundlich equation).

Table 2: Influence of experimental conditions on the parameters of the empirical modeling of breakthrough curves (Eq. 1).

Exper. Run	C_o (mg L^{-1})	U_o (m h^{-1})	Z (cm)	d_c (mm)	d_p (µm)	Comp. Ion (M)	BV^0	$\alpha\ 10^3$
1	5	0.65	4.5	7	125-250	-	9498.3	1.1124
2	25	0.65	4.5	7	125-250	-	2049.1	7.6944
3	50	0.65	4.5	7	125-250	-	1194.0	13.110
4	50	0.37	4.5	7	125-250	-	1159.5	14.126
5	50	1.57	4.5	7	125-250	-	1157.3	13.553
6	50	0.65	2.4	7	125-250	-	1069.4	12.497
7	50	0.65	6.6	7	125-250	-	1204.4	15.944
8	50	0.65	2.3	10	125-250	-	1078.6	12.144
9	50	0.65	6.7	7	250-500	-	884.1	20.47
10	50	0.65	4.5	7	125-250	0.1 Cl^-	815.55	18.103
11	50	0.65	4.5	7	125-250	0.2 NO_3^-	980.00	9.8712
12	50	0.65	4.5	7	125-250	0.1 SO_4^{2-}	515.94	14.482

enlever les décimales

Table 3: Influence of experimental conditions on the parameters of Bohart-Adams and Hutchins models.

Exper. Run	Z_0 (cm)	s ($h\ m^{-1}$)	s_o (h)	N_0 ($kg\ m^{-3}$)	k ($m^3\ kg^{-1}h^{-1}$)
1	1.26	14613	183.45	62.49	3.21
2	0.84	3152	26.47	67.40	4.45
3	0.85	1837	15.54	78.55	3.79
4	0.81	3134	25.38	76.28	2.32
5	0.84	737	6.23	76.14	9.46
6	0.53	1645	8.70	70.36	6.77
7	1.01	1853	18.75	79.24	3.14
8	0.52	1659	8.58	70.96	6.86
9	1.09	557	14.83	21.04	3.97
10	0.90	1255	11.26	53.66	5.23
11	1.37	1508	20.66	64.47	2.85
12	1.78	794	14.09	33.94	4.18

Table 4: Influence of experimental conditions on sorbent usage rate (SUR: g L^{-1}, sorbent mass/breakthrough volume) and degree of sorbent usage (DoSU: %, palladium mass sorbed at exhaustion/mass sorbed at exhaustion).

Exper. Run	EBCT (min)	V_{brk} (mL)	V_{exh} (mL)	q_{brk} (mg g^{-1})	q_{exh} (mg g^{-1})	SUR (g L^{-1})	DoSU (%)
1	4.15	9183	19920	87.9	150.7	0.054	58
2	4.15	2843	4261	137.0	177.4	0.176	77
3	4.15	1699	2683	164.0	198.2	0.294	83
4	7.30	1586	2191	157.0	190.4	0.315	82
5	1.72	1587	2275	151.9	184.0	0.315	83
6	2.22	775	1069	185.1	213.0	0.323	87
7	6.09	2547	3479	164.9	197.6	0.294	83
8	2.12	1507	2356	137.2	176.5	0.332	78
9	6.18	1913	2610	185.4	208.5	0.261	89
10	4.15	1095	1597	102.5	129.2	0.457	79
11	4.15	1274	2537	125.2	165.0	0.392	76
12	4.15	667	1764	63.2	91.7	0.750	69